DOR: 20.1001.1.27170314.2021.10.4.5.0

Research Paper

Temperature-dependent Vibration Analysis of Clamped-free Sandwich Beams with Porous FG Core

Mohsen Rahmani[1*]
[1]Department of Mechanics, Tuyserkan Branch, Islamic Azad University, Tuyserkan, Iran
[*]Email of Corresponding Author: Mohsen_rahmani@ymail.com
Received: December 5, 2021; Accepted: January 29, 2022

Abstract
In recent years, there has been a demand for the production of materials with high thermal resistance and manufacturing structures with high mechanical strength in modern industries. In this paper, the frequency responses analysis of the sandwich beams with functionally graded core and homogeneous face sheets are presented based on the high-order sandwich beam theory. All materials are temperature dependent and the properties of FGM are varied gradually by a power-law rule which is modified by considering even and uneven porosity distributions across the thickness. Nonlinear Lagrange strain and thermal stresses of the face sheets and in-plane strain and transverse flexibility of the core are considered. Governing equations of the motion are obtained based on Hamilton's principle and solved by a Galerkin method for the clamped-free boundary condition. To verify the results of this study, they compared with special cases of the literature. Based on the numerical results, it is concluded that by increasing the temperature, power-law index, length, thickness, porosity volume fraction the fundamental frequency parameter decreases, and increasing the wave number causes the frequency increases.

Keywords
Sandwich Beam, FG Core, Porosity, Temperature-dependent, Clamped-free

1. Introduction

Nowadays, the sandwich panels which usually have two thin and stiff faces and a lightweight flexible core, have become common and useful structures in modern industries such as aerospace, transportation, naval, and construction structures. These structures have a high bending rigidity, high performance with a low weight concurrently [1].

On the other hand, the failure, delamination, and thermal stress concentration are the results of using the classical composite materials in high-temperature environments. To avoid these damages functionally graded materials (FGMs) have been proposed which are microscopic inhomogeneous materials and gradually graded from a metal surface to a ceramic one [2]. In recent years, there has been a demand for the production of materials with high thermal resistance and manufacturing structures with high mechanical strength in modern industries such as aerospace, turbine, reactor, and other machines. The FGMs are modern materials applied in the sandwich structures as coating layers to save the panels in high thermal conditions. There are different methods of manufacturing the FGMs

such as powder densification processes, coating processes, plasma spray forming, thermal spray techniques, laser cladding, settling and centrifugal separation, infiltration processing. In some production processes of FGM, due to technical problems, some micro voids and porosities appear which reduce the mechanical properties such as density and Young modulus. So this important effect must be considered in the model of FGMs.

In the classical theories, the core has been considered as a constant thickness layer, but to investigate the localized effects in the sandwich structures behavior, the high order sandwich panels theory is presented which the core is considered as a transversely flexible layer [3]. Many researchers have been studied the mechanical behaviors of sandwich beams by using different theories.

Fazzolari studied the vibration and elastic stability of functionally graded sandwich beams resting on the elastic foundation by using a higher beam theory [4]. Based on the Timoshenko beam theory, Chen et al. studied the nonlinear vibration of sandwich beam with porous FG core and solved the equation by applying the Ritz method theory [5]. Akbaş investigated the vibration of the FG porous deep beam based on a finite element procedure under thermal conditions [6]. Bourada et al. studied the vibration of FG beams with porosity based on a high order trigonometric deformation theory [7]. Li et al. studied the nonlinear vibration of FG sandwich beams with negative Poisson's ratio honeycomb core based on the 3D full-scale finite element analyses [8]. Wu et al. surveyed the vibration and buckling of sandwich beams with FG carbon nanotube-reinforced composite faces based on the Timoshenko beam theory [9]. Xu et al. investigated vibration of composite sandwich beam with corrugated core based on the continuous homogeneous theory and Rayleigh-Ritz method [10]. Li et al. investigated the vibration of multilayer lattice sandwich beams numerically and experimentally [11]. Li investigated the nonlinear vibration and stability of axially moving viscoelastic sandwich beam under resonances by using the Galerkin method [12]. Şimşek and Al-shujairi investigated different types of vibration behaviors of FG sandwich beams under the harmonic loads by using the Timoshenko beam theory [13]. Nguyen et al. studied the buckling and vibration behaviors of different types of FG sandwich beams by using a quasi 3D beam theory [14]. By using a finite element model, Kahya and Turan investigated the buckling and vibration of different types of FG sandwich beams based on the first-order shear deformation theory [15]. Tossapanon and Wattanasakulpong studied the buckling and vibration behavior of sandwich beams with FG faces resting on elastic foundation based on the Timoshenko beam theory and Chebyshev collocation [16]. Arikoglu and Ozkol investigated the vibration of composite sandwich beams with viscoelastic core based on the differential transform method [17]. Pradhan and Murmu investigated the vibration of FG beams and FG sandwich beams resting on elastic foundations by using the differential quadrature method [18]. Mashat et al. studied the vibration of FG layered beams by using Carrera unified formulation and FEM [19]. Nguyen et al. studied the vibration and buckling of FG sandwich beams based on the higher order shear deformation theory [20]. Vo et al. studied the vibration and buckling of FG sandwich beams by using a quasi 3D theory and a finite element model [21]. Yang et al. studied the vibration behavior of the different type of the FG sandwich beams by using a meshfree boundary-domain integral equation method [22]. Mayandi and Jeyaraj studied the mechanical behaviors of FG-CNTR polymer composite beam such as buckling by using finite element method [23]. Mammano and Dragoni presented the approximate equations of buckled beam based on the elastica solution for low-stiffness elastic suspensions [24]. Alijani and et al. studied the elasto-plastic nonlinear buckling

responses of FGM beams based on the finite element method [25]. Majumdar and Das analyzed the thermal buckling behavior of clamped FG beams based on the Euler-Bernoulli theory [26]. Koissin et al. studied the physical nonlinearity effect on the buckling responses of the sandwich beam with a foam core experimentally, theoretically, and numerically [27]. Tran et al. studied the bending and buckling behavior of sandwich FG beam based on third-order shear deformation theory and finite element method in thermal conditions [28]. Osofero et al. investigated the vibration and buckling of FG sandwich beams by using a quasi-3D theory [29]. Challamel and Girhammar studied the buckling behavior of partial composite beam-columns by using the variational theories and by considering the shear and axial effects [30].

In this study, by using a high order sandwich beam theory modified by considering the flexibility of the core in the thickness direction, free vibration of sandwich beams is investigated. The sandwiches consist of two homogeneous faces which cover an FG core. All materials are temperature dependent and the properties of the FGM are location-dependent which is graded according to a power-law rule. To increase the accuracy of the model of the FGM properties, even and uneven porosity distributions are applied. Nonlinear Lagrange strain and thermal stresses of the face sheets and in-plane strain of the core are considered. Governing equations of the motion are obtained based on Hamilton's principle and solved by a Galerkin method for the clamped-free boundary condition. To validate the present approach, special cases of the results of this analytical approach are compared with some studies. Finally, the effects of temperature, the volume fraction distribution of FGM, some geometrical parameters, and porosity effects on the vibration characteristics of defined sandwich beams are investigated.

2. Formulation

A sandwich beam with a porous FG core is covered by the homogeneous face sheets. A schematic cross-section of this sandwich beam is shown in Figure 1.

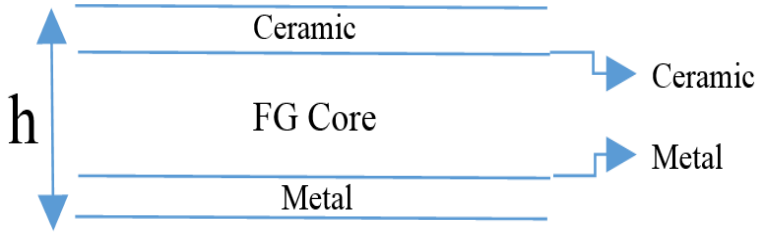

Figure 1. A schematic of sandwich beam

The properties of the homogeneous and the FG materials are temperature dependent which defined as follows [31]:

$$P = P_0\left(P_{-1}T^{-1} + 1 + P_1T + P_2T^2 + P_3T^3\right) \quad (1)$$

Where "P"s are the coefficients of temperature, and they are unique for each material; $T=T_0+\Delta T$, which T_0 is equal to 300(K). Usually, it is considered that functionally graded materials are composed of metal and ceramic. Material properties such as Young's modulus, density, Poisson's ratio are varied gradually across the thickness direction. The power-law rule which consists of even porosity distribution is presented for the FG core as follow [32]:

$$P_c\left(z_c,T\right)=g\left(z_c\right)P_{ce}^c\left(T\right)+\left[1-g\left(z_c\right)\right]P_m^c\left(T\right)-\left(P_{ce}^c\left(T\right)+P_m^c\left(T\right)\right)\frac{\zeta}{2} \quad (2)$$

$$g\left(z_c\right)=\left(\frac{\frac{h_c}{2}-z_c}{h_c}\right)^N \quad (3)$$

where "N" is the constant power-law index; g(z) and [1-g(z)] are volume fraction of ceramic and metal; "ζ" is the porosity distribution; subscripts “m” and “ce” are metal and ceramic and subscripts; "c" refers to the core. In the uneven case, the microvoids are spread in the middle area of the layers decrease near to the edges and tend to zero. So, the power-law rule in the uneven case is modified as follows [32]:

$$P_c\left(z_c,T\right)=g\left(z_c\right)P_{ce}^c\left(T\right)+\left[1-g\left(z_c\right)\right]P_m^c\left(T\right)-\left(P_{ce}^c\left(T\right)+P_m^c\left(T\right)\right)\frac{\zeta}{2}\left(1-\frac{2\left|z_c\right|}{h}\right) \quad (4)$$

To model the displacement fields of the face-sheets, First Order Shear Deformation Theory (FSDT) is employed as follows [33]:

$$u_j\left(x,z,t\right)=u_{0j}\left(x,t\right)+z_j\phi_j\ ;j=\left(t,b\right) \quad (5)$$

$$w_j\left(x,z,t\right)=w_{0j}\left(x,t\right) \quad (6)$$

where "0" denotes values with correspondence to the central plane of the layers; subscripts "t" and "b" refer to the top and bottom faces, respectively "u" and "w" are the in-plane deformation and the transverse deflections of the faces in the "x" and "z" directions, respectively. "Φ" is the rotation of the transverse normal line. Also, the kinematic relations of the core are considered as a polynomial pattern with the unknown coefficients, u_k (k=0,1,2,3), for the in-plane and w_l (l=0,1,2) for vertical displacement components which obtained by the variational principle [34]:

$$u_c\left(x,z_c,t\right)=u_0\left(x,t\right)+u_1\left(x,t\right)z_c+u_2\left(x,t\right)z_c^2+u_3\left(x,t\right)z_c^3 \quad (7)$$

$$w_c\left(x,z_c,t\right)=w_0\left(x,t\right)+w_1\left(x,t\right)z_c+w_2\left(x,t\right)z_c^2 \quad (8)$$

In this theory, the compatibility conditions assume that the faces are stuck to the core completely and the interface displacements between the core and the face sheets can be obtained as follows [35]:

$$u_c\left(z_c=-h_c/2\right)=u_t\left(z_t=h_t/2\right),\ w_c\left(z_c=-h_c/2\right)=w_t \quad (9)$$

$$u_b\left(z_b=-h_b/2\right)=u_c\left(z_c=h_c/2\right),\ w_b=w_c\left(z_c=h_c/2\right) \quad (10)$$

To obtain the governing equations of the motion, Hamilton's energy principle is applied as follow:

$$\int_{t1}^{t2}\left(-\delta K+\delta U\right)dt=0 \quad (11)$$

The variation of kinetic and the strain energy are "δK" and "δU", respectively; "t" is the time coordinate that varies between the times "t_1" and "t_2"; "δ" is the variation operator. The variation of the kinetic energy is calculated as follows:

$$\int_{t1}^{t2}\delta K dt = -\int_{t1}^{t2}\{\int_0^L\int_{-\frac{h_t}{2}}^{\frac{h_t}{2}}\rho_t\left(z_t\right)(\ddot{u}_t\delta u_t+\ddot{w}_t\delta w_t)dxdz_t+\int_0^L\int_{-\frac{h_b}{2}}^{\frac{h_b}{2}}\rho_b\left(z_b\right)(\ddot{u}_b\delta u_b+\ddot{w}_b\delta w_b)dxdz_b$$
$$+\int_0^L\int_{-\frac{h_c}{2}}^{\frac{h_c}{2}}\rho_c(\ddot{u}_c\delta u_c+\ddot{w}_c\delta w_c)dxdz_c\}dt \tag{12}$$

where (··) indicates the second derivative to time; The density is "ρ" which in the functionally graded layers is the function of the displacement. The variation of the total strain energy in the face sheets and the core, also the compatibility conditions at the interfaces of the layers which are the constraints and attended in Hamilton's principle in terms of Lagrange multipliers, is expressed as follows:

$$\delta U_p=\int_{A_t}(\sigma_{xx}^t\delta\varepsilon_{xx}^t+\sigma_{xx}^{tT}\delta d_{xx}^t+\tau_{xz}^t\delta\gamma_{xz}^t+\sigma_{zz}^{tT}\delta d_{zz}^t)dA+\int_{A_b}(\sigma_{xx}^b\delta\varepsilon_{xx}^b+\sigma_{xx}^{bT}\delta d_{xx}^b+\tau_{xz}^b\delta\gamma_{xz}^b+\sigma_{zz}^{bT}\delta d_{zz}^b)dA+$$
$$\int_{A_{core}}(\sigma_{xx}^c\delta\varepsilon_{xx}^c+\sigma_{zz}^c\delta\varepsilon_{zz}^c+\tau_{xz}^c\delta\gamma_{xz}^c)dA+\delta\int_0^L[\lambda_{xt}\left(\mathrm{u_t}\left(z_t=\frac{h_t}{2}\right)-u_c\left(z_c=-\frac{h_c}{2}\right)\right)+ \tag{13}$$
$$\lambda_{zt}\left(\mathrm{w_t}-\mathrm{w_c}\left(z_c=-\frac{h_c}{2}\right)\right)+\lambda_{xb}(\mathrm{u_c}\left(z_c=\frac{h_c}{2}\right)-u_b\left(z_b=-\frac{h_b}{2}\right)+\lambda_{zb}\left(\mathrm{w_c}\left(z_c=\frac{h_c}{2}\right)-w_b\right)]dx$$

where "σ_{xx}" is the in-plane normal stress; "τ_{xz}" is the in-plane shear stresses; "ε_{xx}" and "γ_{xz}" display the in-plane normal and shear linear strains; "d_{xx}" and "d_{zz}" are the in-plane normal and shear nonlinear strains of the layers; "σ^T_{xx}" and "σ^T_{zz}" express the thermal stresses; "σ^c_{zz}" and "ε^c_{zz}" present the lateral normal stress and strain in the core; "τ^c_{xz}" and "γ^c_{xz}" declare shear stress and shear strain in the core; and "λ_x' and "λ_z" are the Lagrange multipliers.

Considering small deflection, the strain components for the faces can be declared as follows [36]:

$$\varepsilon_{xx}^j=u_{j,x},\ j=(t,b) \tag{14}$$

$$d_{xx}^j=+\frac{1}{2}\left(w_{j,x}\right)^2-\alpha_j\Delta T_j \tag{15}$$

$$\gamma_{xz}^j\left(x,z_j,t\right)=\phi_j(x,t)+w_{j0,x}(x,t) \tag{16}$$

$$d_{zz}^j=\frac{1}{2}\phi_{jx}^2-\alpha_j\Delta T_j \tag{17}$$

The"(),i" expresses derivation with respect to "i". The strain of the core can be defined as [36]:

$$\varepsilon_{xx}^c\left(x,z_c,t\right)=u_{c,x}\left(x,z_c,t\right) \tag{18}$$

$$\gamma_{xz}^c\left(x,z_c,t\right)=u_{c,z}\left(x,z_c,t\right)+ w_{c,x}\left(x,z_c,t\right) \tag{19}$$

$$\varepsilon_{zz}^c\left(x,z_c,t\right)=w_{c,z}\left(x,z_c,t\right) \tag{20}$$

In this model by substituting the expressions of the Eq. (12) and Eq. (13) according to the kinematic relations of the layers and using the interfaces relations, and after some algebraic operations, the

thirteen equations of motion are obtained. These equations are not independent and by using the compatibility conditions and based on a reduction method the number of equations is reduced to nine. These equations include two unknowns of the faces and seven unknowns of the core which are presented in the follows:

$$\begin{aligned}&+I_{0t}\ddot{u}_{0c}\,h_t/2-I_{1t}\ddot{u}_{0c}-I_{0t}\ddot{\phi}_{0c}\,h_t h_c/4+I_{1t}\ddot{\phi}_{0c}\,h_c/2+I_{0t}\ddot{u}_{2c}\,h_t h_c^2/8-I_{1t}\ddot{u}_{2c}\,h_c^2/4\\&-I_{0t}\ddot{u}_{3c}\,h_t h_c^3/16+I_{1t}\ddot{u}_{3c}\,h_c^3/8-I_{0t}\ddot{\phi}_t\,h_t^2/4+I_{1t}\ddot{\phi}_t h_t-I_{2t}\ddot{\phi}_t+h_t/2N^{t}_{xx,x}-M^{t}_{xx,x}\\&+N^{t}_{xz}+N^{tT}_{zz}\phi_t=0\end{aligned}\tag{21}$$

$$\begin{aligned}&-I_{0b}\ddot{u}_{0c}\,h_b/2-I_{1b}\ddot{u}_{0c}-I_{0b}\ddot{\phi}_{0c}\,h_b h_c/4-I_{1b}\ddot{\phi}_{0c}\,h_c/2-I_{0b}\ddot{u}_{2c}\,h_b h_c^2/8-I_{1b}\ddot{u}_{2c}\,h_c^2/4-\\&I_{0b}\ddot{u}_{3c}\,h_b h_c^3/16-I_{1b}\ddot{u}_{3c}\,h_c^3/8-I_{0b}\ddot{\phi}_b\,h_b^2/4-I_{1b}\ddot{\phi}_b h_b-I_{2b}\ddot{\phi}_b-h_b/2N^{b}_{xx,x}-\\&M^{b}_{xx,x}+N^{b}_{xz}+N^{bT}_{zz}\phi_b=0\end{aligned}\tag{22}$$

$$\begin{aligned}&-I_{0t}\ddot{u}_{0c}+I_{0t}\ddot{\phi}_{0c}\,h_c/2-I_{0t}\ddot{u}_{2c}\,h_c^2/4+I_{0t}\ddot{u}_{3c}\,h_c^3/8+I_{0t}\ddot{\phi}_t\,h_t/2-I_{1t}\ddot{\phi}_t\\&-I_{0b}\ddot{u}_{0c}-I_{0b}\ddot{\phi}_{0c}\,h_c/2-I_{0b}\ddot{u}_{2c}\,h_c^2/4-I_{0b}\ddot{u}_{3c}\,h_c^3/8-I_{0b}\ddot{\phi}_b\,h_b/2-I_{1b}\ddot{\phi}_t\\&-I_{0c}\ddot{u}_{0c}-I_{1c}\ddot{\phi}_{0c}-I_{2c}\ddot{u}_{2c}-I_{3c}\ddot{u}_{3c}-N^{t}_{xx,x}-N^{b}_{xx,x}-R^{c}_{x,x}=0\end{aligned}\tag{23}$$

$$\begin{aligned}&+I_{0t}\ddot{u}_{0c}\,h_c/2-I_{0t}\ddot{\phi}_{0c}\,h_c^2/4+I_{0t}\ddot{u}_{2c}\,h_c^3/8-I_{0t}\ddot{u}_{3c}\,h_c^4/16-I_{0t}\ddot{\phi}_t\,h_t h_c/4+I_{1t}\ddot{\phi}_t\,h_c/2\\&-I_{0b}\ddot{u}_{0c}\,h_c/2-I_{0b}\ddot{\phi}_{0c}\,h_c^2/4-I_{0b}\ddot{u}_{2c}\,h_c^3/8-I_{0b}\ddot{u}_{3c}\,h_c^4/16-I_{0b}\ddot{\phi}_b\,h_b h_c/4-I_{1b}\ddot{\phi}_b\,h_c/2\\&-I_{1c}\ddot{u}_{0c}-I_{2c}\ddot{\phi}_{0c}-I_{3c}\ddot{u}_{2c}-I_{4c}\ddot{u}_{3c}+h_c/2N^{t}_{xx,x}-h_c/2N^{b}_{xx,x}-M^{c}_{x1,x}+Q^{c}_{xz}=0\end{aligned}\tag{24}$$

$$\begin{aligned}&-I_{0t}\ddot{u}_{0c}\,h_c^2/4+I_{0t}\ddot{\phi}_{0c}\,h_c^3/8-I_{0t}\ddot{u}_{2c}\,h_c^4/16+I_{0t}\ddot{u}_{3c}\,h_c^5/32+I_{0t}\ddot{\phi}_t\,h_t h_c^2/8-I_{1t}\ddot{\phi}_t\,h_c^2/4\\&-I_{0b}\ddot{u}_{0c}\,h_c^2/4-I_{0b}\ddot{\phi}_{0c}\,h_c^3/8-I_{0b}\ddot{u}_{2c}\,h_c^4/16-I_{0b}\ddot{u}_{3c}\,h_c^5/32-I_{0b}\ddot{\phi}_b\,h_b h_c^2/8\\&-I_{1b}\ddot{\phi}_b\,h_c^2/4-I_{2c}\ddot{u}_{0c}-I_{3c}\ddot{\phi}_{0c}-I_{4c}\ddot{u}_{2c}-I_{5c}\ddot{u}_{3c}-h_c^2/4N^{t}_{xx,x}-h_c^2/4N^{b}_{xx,x}\\&-M^{c}_{x2,x}+2M^{c}_{Q1xc}=0\end{aligned}\tag{25}$$

$$\begin{aligned}&+I_{0t}\ddot{u}_{0c}\,h_c^3/8-I_{0t}\ddot{\phi}_{0c}\,h_c^4/16+I_{0t}\ddot{u}_{2c}\,h_c^5/32-I_{0t}\ddot{u}_{3c}\,h_c^6/64-I_{0t}\ddot{\phi}_t\,h_t h_c^3/16\\&+I_{1t}\ddot{\phi}_t\,h_c^3/8-I_{0b}\ddot{u}_{0c}\,h_c^3/8-I_{0b}\ddot{\phi}_{0c}\,h_c^4/16-I_{0b}\ddot{u}_{2c}\,h_c^5/32-I_{0b}\ddot{u}_{3c}\,h_c^6/64\\&-I_{0b}\ddot{\phi}_b\,h_b h_c^3/16-I_{1b}\ddot{\phi}_b\,h_c^3/8-I_{3c}\ddot{u}_{0c}-I_{4c}\ddot{\phi}_{0c}-I_{5c}\ddot{u}_{2c}-I_{6c}\ddot{u}_{3c}+h_c^3/8N^{t}_{xx,x}\\&-h_c^3/8N^{b}_{xx,x}-M^{c}_{x3,x}+3M^{c}_{Q2xc}=0\end{aligned}\tag{26}$$

$$\begin{aligned}&-I_{0t}\ddot{w}_{0c}+I_{0t}\ddot{w}_{1c}\,h_c/2-I_{0t}\ddot{w}_{2c}-I_{0b}\ddot{w}_{0c}-I_{0b}\ddot{w}_{1c}\,h_c/2-I_{0b}\ddot{w}_{2c}\,h_c^2/4-\\&I_{0c}\ddot{w}_{0c}-I_{1c}\ddot{w}_{0c}-I_{2c}\ddot{w}_{2c}-N^{t}_{xz,x}-N^{b}_{xz,x}-Q^{c}_{xz,x}-N^{tT}_{xx,x}w_{0c,x}-N^{tT}_{xx}w_{0c,xx}+\\&N^{tT}_{xx,x}w_{1c,x}\,h_c/2+N^{tT}_{xx}w_{1c,xx}\,h_c/2-N^{tT}_{xx,x}w_{2c,x}\,h_c^2/4-N^{tT}_{xx}w_{2c,xx}\,h_c^2/4-\\&N^{bT}_{xx,x}w_{0c,x}-N^{bT}_{xx}w_{0c,xx}-N^{bT}_{xx,x}w_{1c,x}\,h_c/2-N^{bT}_{xx}w_{1c,xx}\,h_c/2-N^{bT}_{xx,x}w_{2c,x}\,h_c^2/4\\&-N^{bT}_{xx}w_{2c,xx}\,h_c^2/4=0\end{aligned}\tag{27}$$

$$\begin{aligned}&+I_{0t}\ddot{w}_{0c}\,h_c/2-I_{0t}\ddot{w}_{1c}\,h_c^2/4+I_{0t}\ddot{w}_{2c}\,h_c^3/8-I_{0b}\ddot{w}_{0c}\,h_c/2-I_{0b}\ddot{w}_{1c}\,h_c^2/4-\\&I_{0b}\ddot{w}_{2c}\,h_c^3/8-I_{1c}\ddot{w}_{0c}-I_{2c}\ddot{w}_{0c}-I_{3c}\ddot{w}_{2c}+h_c/2N^{t}_{xz,x}-h_c/2N^{b}_{xz,x}-M^{c}_{Q1xc,x}\\&+R^{c}_{z}-N^{tT}_{xx,x}w_{1c,x}\,h_c^2/4-N^{tT}_{xx}w_{1c,xx}\,h_c^2/4+N^{tT}_{xx,x}w_{0c,x}\,h_c/2+N^{tT}_{xx}w_{0c,xx}\,h_c/2+\\&N^{tT}_{xx,x}w_{2c,x}\,h_c^3/8+N^{tT}_{xx}w_{2c,xx}\,h_c^3/8-N^{bT}_{xx,x}w_{1c,x}\,h_c^2/4-N^{bT}_{xx}w_{1c,xx}\,h_c^2/4-\\&N^{bT}_{xx,x}w_{0c,x}\,h_c/2-N^{bT}_{xx}w_{0c,xx}\,h_c/2-N^{bT}_{xx,x}w_{2c,x}\,h_c^3/8-N^{bT}_{xx}w_{2c,xx}\,h_c^3/8=0\end{aligned}\tag{28}$$

$$\begin{aligned}&-I_{0t}\ddot{w}_{0c}\,h_c^2/4+I_{0t}\ddot{w}_{1c}\,h_c^3/8-I_{0t}\ddot{w}_{2c}\,h_c^4/16-I_{0b}\ddot{w}_{0c}\,h_c^2/4-I_{0b}\ddot{w}_{1c}\,h_c^3/8\\&-I_{0b}\ddot{w}_{2c}\,h_c^4/16-I_{2c}\ddot{w}_{0c}-I_{3c}\ddot{w}_{0c}-I_{4c}\ddot{w}_{2c}-h_c^2/4N^{t}_{xz,x}-h_c^2/4N^{b}_{xz,x}\\&-M^{c}_{Q2xc,x}+2M^{c}_{z}-N^{tT}_{xx,x}w_{2c,x}\,h_c^4/16-N^{tT}_{xx}w_{2c,xx}\,h_c^4/16-N^{tT}_{xx,x}w_{0c,x}\,h_c^2/4-\\&N^{tT}_{xx}w_{0c,xx}\,h_c^2/4+N^{tT}_{xx,x}w_{1c,x}\,h_c^3/8+N^{tT}_{xx}w_{1c,xx}\,h_c^3/8-N^{bT}_{xx,x}w_{2c,x}\,h_c^4/16-\\&N^{bT}_{xx}w_{2c,xx}\,h_c^4/16-N^{bT}_{xx,x}w_{0c,x}\,h_c^2/4-N^{bT}_{xx}w_{0c,xx}\,h_c^2/4-N^{bT}_{xx,x}w_{1c,x}\,h_c^3/8-\\&N^{bT}_{xx}w_{1c,xx}\,h_c^3/8=0\end{aligned}\tag{29}$$

$$u_{0t}+\frac{h_t}{2}\phi^t=u_{0c}-\frac{h_c}{2}\phi_0^c+\frac{h_c^2}{4}u_{2c}-\frac{h_c^3}{8}u_{3c}=0\tag{30}$$

$$w_{0t} = +w_{0c} - \mathrm{h_c}/2\, w_{1c} + \mathrm{h_c}^2/4\, w_{2c} \tag{31}$$

$$u_{0b} - \frac{h_b}{2}\phi^b = u_{0c} + \frac{h_c}{2}\phi_0^c + \frac{h_c^2}{4}u_{2c} + \frac{h_c^3}{8}u_{3c} = 0 \tag{32}$$

$$w_{0b} = +w_{0c} + \mathrm{h_c}/2\, w_{1c} + \mathrm{h_c}^2/4\, w_{2c} \tag{33}$$

where "I_{kt}", "I_{kb}" (k=0, 1, 2) are the inertia terms of the top and the bottom face sheets, respectively; "I_{lc}" (l=0, 1…6) are the inertia terms of the core. "N^j_{xx}", "N^j_{xz}", (j=t, b) are the stress resultants and "M^j_{xx}" (j=t, b) is the moment resultants of the top and the bottom face sheets; "N^{jT}_{xx}", "N^{jT}_{zz}",(j=t, b) are the force thermal resultants; "Q_{xc}", "M_{Q1xc}", "M_{Q2xc}", "R_{zc}", "M_{zc}", "R_{xc}", "M_{x1c}", "M_{x2c}" and "M_{x3c}" are the high order stress resultant of the core. In the relations of the face sheets, the in-plane stress resultants, "N_{xx}"; the moment resultants, "M_{xx}"; and then out of plane shear stress resultants, "N_{xz}", is calculated as follows [36]:

$$N^{\,j}_{xx} = A_{11}u^j_{0,x} + B_{11}\phi^j_{,x} - N^{\,jT}_{xx}\,,\ j = (t,b) \tag{34}$$

$$M^{\,j}_{xx} = B_{11}u^j_{0,x} + D_{11}\phi^j_{,x} - M^{\,jT}_{xx} \tag{35}$$

$$N^{\,j}_{xz} = \pi^2/_{12} A_{44}(\phi^j + w^{\,j}_{0,x}) \tag{36}$$

"A" is the stretching stiffness, "B" is the bending-stretching stiffness and "D" is the bending stiffness; which are constant coefficients and express as [37]:

$$\begin{Bmatrix} A^j_{11} \\ B^j_{11} \\ D^j_{11} \end{Bmatrix} = \int_{-hj/2}^{hj/2} \left(\frac{E_j}{1-\nu_j{}^2} \right) \begin{Bmatrix} 1 \\ z_j \\ z_j^{\,2} \end{Bmatrix} dz_j$$
$$\left\{ A^j_{44} \right\} = \int_{-hj/2}^{hj/2} \left(\frac{E_j}{2(1+\nu_j)} \right) dz_j \tag{37}$$

The high order thermal stress resultants in the face sheets are depicted as follows [31]:

$$\left\{ N^{jT}_{xx}, N^{jT}_{zz} \right\} = -\int_{-hj/2}^{hj/2} \left(\frac{E_j}{1-\nu_j} \alpha_j T_j \right) dz_j\ ,\ j = (t,b) \tag{38}$$

where E, ν, and α are Young's modulus, the Poisson's ratio, and the thermal expansion coefficient, respectively, which in the functionally graded layers are the function of the displacement, too. The inertia terms of the face sheets and the core are calculated as follows [36]:

$$\left(I_{0j}, I_{1j}, I_{2j} \right) = \int_{-hj/2}^{hj/2} \rho_j \left(1, z_j, z_j^{\,2} \right) dz_j\,,\ \left(j = t,b \right) \tag{39}$$

$$\left(I_{0c}, I_{1c}, I_{2c}, I_{3c}, I_{4c}, I_{5c}, I_{6c} \right) = \int_{-hc/2}^{hc/2} \rho_c \left(1, z_c, z_c^{\,2}, z_c^{\,3}, z_c^{\,4}, z_c^{\,5}, z_c^{\,6} \right) dz_c \tag{40}$$

The high order stress resultants of the core are as follows:

$$Q_{xc}, M_{Q1xc}, M_{Q2xc} = \int_{-hc/2}^{hc/2} \left(1, z_c, z_c^2 \right) \sigma^c_{xz} dz_c \tag{41}$$

$$R_{zc}, M_{zc} = \int_{-hc/2}^{hc/2} \left(1, z_c \right) \sigma^c_{zz} dz_c \tag{42}$$

$$R^c_x, M^c_{x1}, M^c_{x2}, M^c_{x3} = \int_{-hc/2}^{hc/2} \left(1, z_c, z_c^2, z_c^3 \right) \sigma^c_{xx} dz_c \tag{43}$$

Finally, by substituting the high order stress resultants in terms of the kinematic relations, the equations are derived in terms of the nine unknowns.

3. Verification and Numerical Results

To solve the equations of the free vibration of the FG sandwich beam, a Galerkin method with nine trigonometric shape functions, which satisfy the boundary condition, is established. The shape functions of the clamped-free boundary condition can be expressed as [38]:

$$\phi_x^j = C_{\phi xj}\frac{\lambda_m}{L}(\sinh(\frac{\lambda_m x}{L})+\sin(\frac{\lambda_m x}{L})-\gamma_m(\cos h(\frac{\lambda_m x}{L})-\cos(\frac{\lambda_m x}{L})))e^{i\omega t},\ j=(t,b) \tag{44}$$

$$u_{ck} = C_{uk}\frac{\lambda_m}{L}(\sinh(\frac{\lambda_m x}{L})+\sin(\frac{\lambda_m x}{L})-\gamma_m(\cos h(\frac{\lambda_m x}{L})-\cos(\frac{\lambda_m x}{L})))e^{i\omega t},\ k=(0,1,2,3) \tag{45}$$

$$w_{ck} = C_{wk}(\cosh(\frac{\lambda_m x}{L})-\cos(\frac{\lambda_m x}{L})-\gamma_m(\sin h(\frac{\lambda_m x}{L})-\sin(\frac{\lambda_m x}{L})))e^{i\omega t},\ k=(0,1,2) \tag{46}$$

$$\cos\lambda_m.\cosh\lambda_m=-1;\ \lambda_m=1.875,4.694,7.854,10.995,14.137 \tag{47}$$

$$\gamma_m=\frac{\sinh\lambda_m-\sin\lambda_m}{\cosh\lambda_m-\cos\lambda_m}\quad m=(1,2,3,...) \tag{48}$$

where "$a_m=m\pi/L$; "m" is the wave number and $C_{uk}, C_{wk}, C_{\phi j}$ are the nine unknown constants of the shape functions. These nine equations can be written in a 9×9 matrix which includes the mass, "M", and stiffness, "K", matrices as follows:

$$(k_m-\omega_m^2 M_m)C_m=0 \tag{49}$$

In Eq. (49), ω_m is the natural frequency; and "C_m" is the eigenvector which contains nine unknown constants.

To validate the approach of this study, present results in a special case are compared with results of literature [39-41] which are shown in Table 1, for the simply supported (S-S) and clamped (C-C) boundary conditions. There is a good agreement between the results. Since the procedure of the present study is different with references [39-41], negligible discrepancies are seen in the results.

Table 1. Fundamental frequency parameters of present results and literature [39-41] (L/h=5)

B.C	reference	N=0	N=0.5	N=1	N=2
S-S	Simsek [39]	5.1525	4.4083	3.9902	3.6344
	Vo [41]	5.1526	4.3990	3.9711	3.6050
	Nguyen [40]	5.1525	4.4075	3.9902	3.6344
	Present method	5.0789	4.3312	3.8618	3.5487
C-C	Simsek [39]	10.0344	8.7005	7.9253	7.2113
	Vo [41]	9.9984	8.6717	7.9015	7.1901
	Present method	9.9151	8.5887	7.8080	7.1088

Consider an FG sandwich beam which is assumed to be made from a mixture of Silicon nitride as ceramic phase and Stainless steel as a metal phase. The temperature-dependent properties of constituent materials which are introduced by Eq. (1) are presented in the reference [33]. For simplicity, the fundamental frequency parameter defined that is non-dimensional as:

$$\bar{\omega}=\omega/1000 \tag{50}$$

In general, the h_t-h_c-h_b sandwich beam is a structure with the indices of outer face sheet thickness, core thickness, and inner face sheet thickness equal to h_t, h_c, and h_b, respectively. Therefore, in a 1-8-1 sandwich, the core thickness is eight times every face sheet thickness.

Temperature variation has an important effect on the frequency of the structures. According to Eq. (1), temperature rising reduces the Young modulus of metal and ceramic. So, the strength of the materials reduces, which is an important reason for decreasing the frequency in high-temperature conditions. Figure 2 shows the fundamental frequency parameter variation versus the temperature for 1-8-1 FG core sandwich beam with clamped-free boundary conditions. Geometrical parameters are "h = 0.02m, L/h=5, m=1". By increasing the temperature, the fundamental frequency parameters decrease. As shown in Figure 2, when N=0, the FG layer is made of full ceramic, as a result, the stability and resistance against the high-temperature conditions are more than the other values of "N", so its fundamental frequency parameters are higher than others. By increasing the power-law index, "N", the amount of the ceramic reduces in the structure which causes the young modulus of the FGM and the stability of the structures to decrease. When "N=0", by increasing the temperature, the fundamental frequency parameter decreases 22.78%, for "N=1" and "N=2" it decreases 34.33%, and 35.23%, respectively.

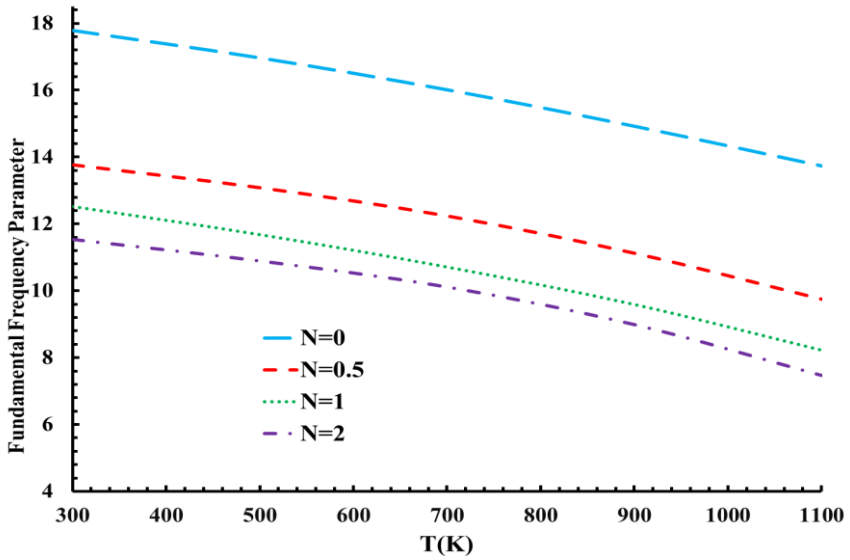

Figure 2. Fundamental frequency variation versus temperature rising

Some geometrical effects on the fundamental frequency of FG sandwich beams are investigated. Figure 3 shows the effect of length to thickness ratio on the fundamental frequency parameter in 1-8-1 FG core sandwich beam in the clamped-free boundary conditions. Geometrical parameters are "h = 0.02m, T=300K, m=1". When ratios are increased in a constant "N", the fundamental frequency parameter decreases. Based on Figure 3, by increasing this ratio, the stability of the structure reduces and it is important to consider that long length is not proper for the FG sandwich beams. Also, it is obvious that by increasing the power-law index, "N", the fundamental frequency parameters decrease, but in this case effect of variation of the length is a dominant parameter and its variation has an impressive effect on the fundamental frequency. For example, for "L/h=5", by increasing "N", the fundamental frequency parameter decreases 35.18%, but for "N=0", by increasing this ratio, the

fundamental frequency decreases 6193%. Also, it should be noted that when the ratio is more than 12, the slope of the variation of the fundamental frequency is decreased significantly.

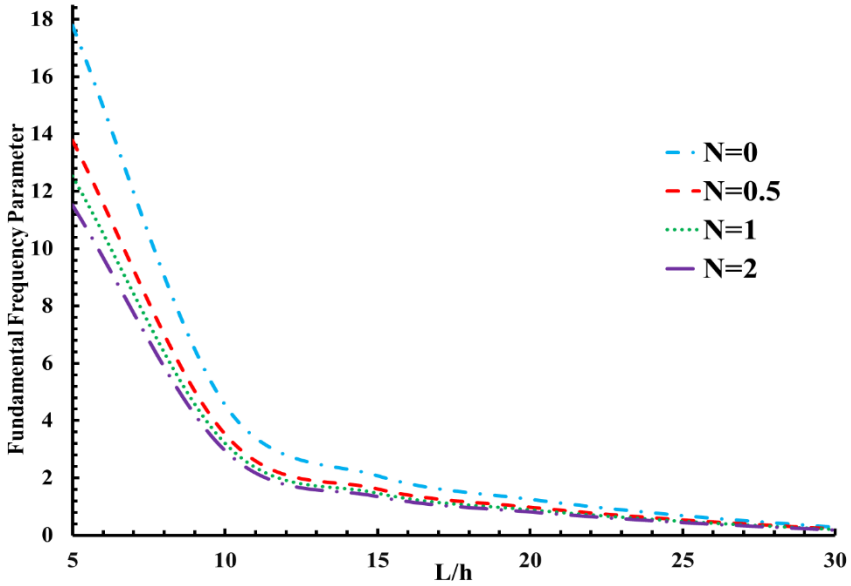

Figure 3. Fundamental frequency variation versus L/h ratio

Figure 4 shows the effect of the variation of the core to face sheet thickness ratio, "h_c/h_t", on the fundamental frequency parameter in various power-law indices and constant total thickness. When "h_c/h_t=0.5", it means the thickness of the faces is two times the core thickness, so it shows the results of the 2-1-2 sandwich. And, when "h_c/h_t=8", it shows results of the 1-8-1 sandwich. Geometrical parameters are "h = 0.02m, T=300K, m=1, L/h=10". By increasing the ratio in a constant total thickness, the amount of ceramic increases, and the structure becomes stiffer, so the fundamental frequency parameters increase at lower gradient indices. Since in 1-8-1 sandwich, the amount of ceramic is more than 2-1-2 one, it is clear that the fundamental frequency parameter is higher, as shown in Figure 4. But from a certain value of the power-law index, by increasing the power-law index, the fundamental frequency of the 2-1-2 becomes more than 1-8-1 sandwiches. By increasing the power-law index in a constant thickness, the ceramic quantity of the FG layer decreases, so, for all values of "h_c/h_t", the fundamental frequency parameters decrease. In "h_c/h_t=0.5", the fundamental frequency parameter decrease 7.626 when "N" is increased, and in "h_c/h_t=8", the fundamental frequency parameter decreases 34.96% when "N" is increased. Also, for "N=0", by increasing this ratio, the fundamental frequency increases 31.50%, but for "N=2", it decreases 7.38%.

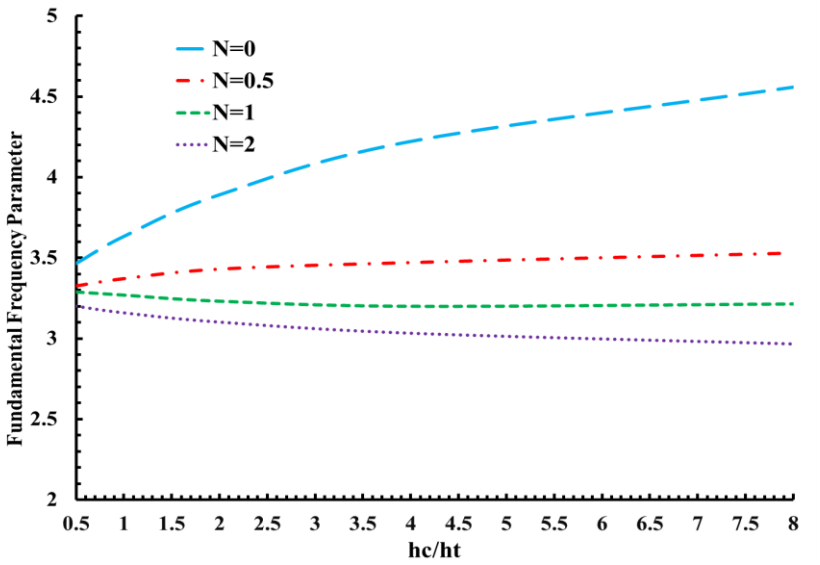

Figure 4. Effect of variation of the core to face sheets thickness ratio on the fundamental frequency parameter

The effect of the variation of the wave number, "m", on the fundamental frequency parameter in various power-law indices and the constant total thickness is depicted in Figure 5. Geometrical parameters are "T=300K, L/h=10". By increasing the wave number, the fundamental frequency parameters increase.

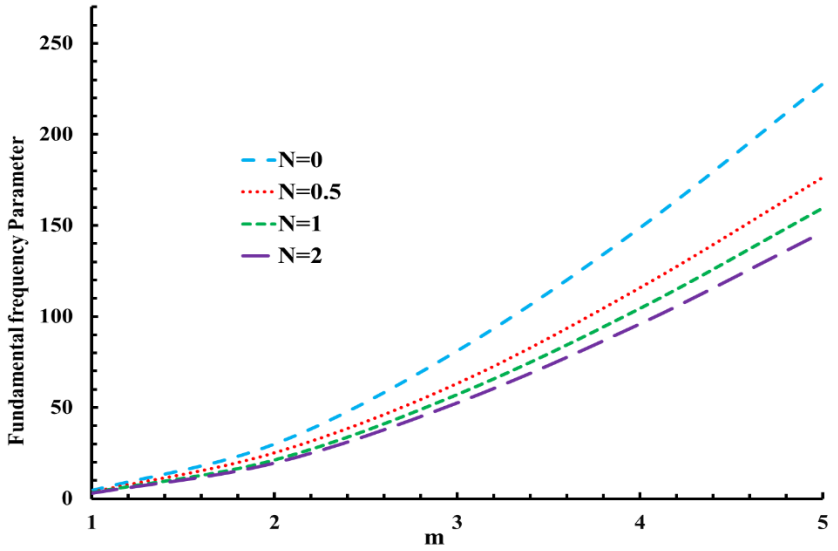

Figure 5. Effect of variation of the wave number on the fundamental frequency parameter

The effect of the variation of the total thickness of the sandwiches, "h", on the fundamental frequency parameter in various power-law indices for clamped-free FG sandwich beam is depicted in Figure 6. It is obvious that by increasing the total thickness in a constant L/h ratio, the fundamental frequency parameter decreases.

The slope of decreasing the frequency in the value of lower than 0.02m is severe, but in the higher values, the slope of decreasing is lower. It means after a certain value, increasing the thickness has a little effect on the frequency. For example, in "N=0" by increasing the "h", the fundamental frequency

parameter decreases 2487.91%. But, it is seen that after the "h=0.02m", the rate of variation is decreased and the difference is 562.99%. For "h=0.01m", by increasing "N", the fundamental frequency parameter decrease 54.27%.

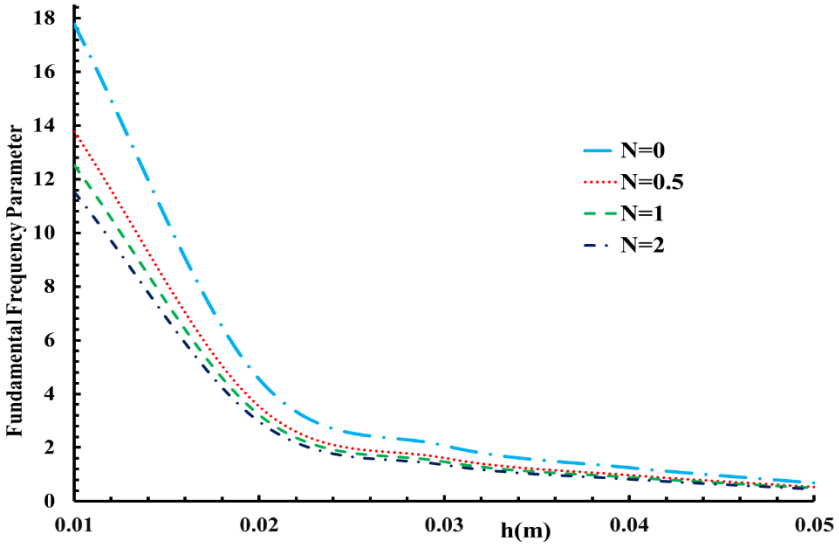

Figure 6. Effect of the variation of the total thickness of the sandwiches on the fundamental frequency parameter

To investigate the porosity influence, Figure 7 and Figure 8 show the effects of even and uneven porosity distributions on the fundamental frequency parameters of sandwich beam, respectively. Geometrical parameters are "h = 0.02m, L/h=10, m=1". In the even distributions, porosities occur all over the cross-section of the FG layer. While, in the uneven distribution, porosities are available at the middle zone of the cross-section. As shown in Figure 7 and Figure 8, by increasing the porosity volume fraction, the fundamental frequency parameters increase for all power-law indices. The slope of increasing is stronger in the case of even porosity distribution. In the even case in "N=0", by increasing the volume fraction of the porosity, the fundamental frequency increases 64.43%, and in the uneven case in "N=0", by increasing the volume fraction of the porosity, the fundamental frequency increases 21.91%.

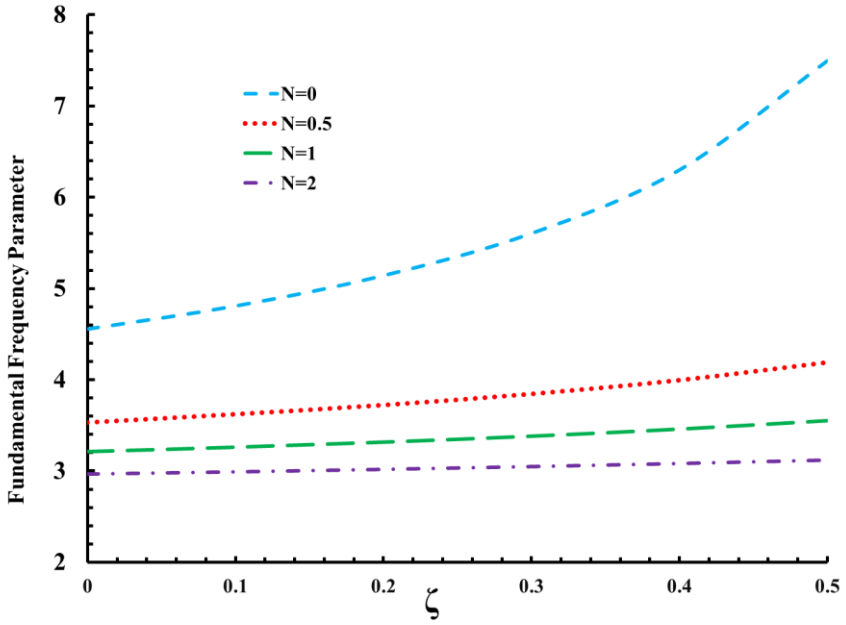

Figure 7. Fundamental frequency variation versus even porosity

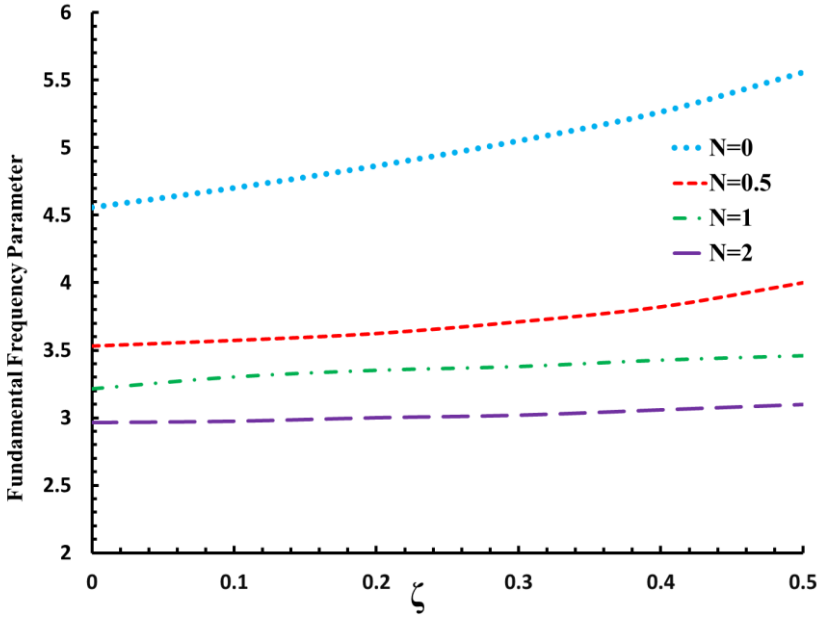

Figure 8. Fundamental frequency variation versus uneven porosity

4. Conclusion

In this study, frequency analysis of the 1-8-1 sandwich beams, according to a high order sandwich beam theory was presented. The fields of the displacement of the face sheets were considered based on the first-order shear deformation theory and the core displacement fields were considered as the polynomial distributions for vertical and horizontal deflections. High order stresses resultants in-plane stresses in the core and thermal stress resultants, and nonlinear strains in the face sheets were considered. All materials were temperature-dependent. A power law distribution was used to model the material properties of the FG core which was modified by considering two distributions of

porosity. The equations of motion were obtained by Hamilton's principal and solved by using the Galerkin method for clamped-free boundary conditions. To survey the capabilities of this model for free vibration analysis, the results were verified by literature results in a special case. Based on the results, there was a good agreement between them. The following conclusion can be drawn:

1. When the temperature is increased, the fundamental frequency parameters decrease.
2. By increasing the power-law index, the amount of ceramic reduces, so the fundamental frequency parameter decreases.
3. By increasing the length to thickness ratio, the stability of the structure reduces, so the fundamental frequency parameter decreases.
4. In a constant total thickness, by increasing the core to face-sheet thickness ratio, first the fundamental frequency parameters increase at the lower gradient indices, but from a certain value of the power-law index, by increasing the power-law index, when the ratio is increased, the fundamental frequency parameters decrease.
5. By increasing the wave number, the fundamental frequency parameter increases.
6. By increasing the total thickness of the sandwich beams, the fundamental frequency parameter decreases.
7. By increasing the porosity volume fraction in both even and uneven distributions, the fundamental frequency parameter increases. Variation of frequencies in even porosity cases is more than uneven cases.

5. References

[1] Vinson, J. 2018. The behavior of sandwich structures of isotropic and composite materials, TECHNOMIC, Pennsylvania.

[2] Rahmani, M., Mohammadi, Y. and Kakavand, F. 2019. Vibration analysis of sandwich truncated conical shells with porous FG face sheets in various thermal surroundings. Steel and Composite Structures. 32(2): 239-252.

[3] Frostig, Y., Baruch, M., Vilnay, O. and Sheinman, I. 1992. High-order theory for sandwich-beam behavior with transversely flexible core. Journal of Engineering Mechanics. 118(5): 1026-1043.

[4] Fazzolari, F. A. 2018. Generalized exponential, polynomial and trigonometric theories for vibration and stability analysis of porous FG sandwich beams resting on elastic foundations. Composites Part B: Engineering. 136:254-271.

[5] Chen, D., Kitipornchai, S. and Yang, J. 2016. Nonlinear free vibration of shear deformable sandwich beam with a functionally graded porous core. Thin-Walled Structures. 107:39-48.

[6] Akbaş, Ş. D. 2017. Thermal effects on the vibration of functionally graded deep beams with porosity. International Journal of Applied Mechanics. 9(05): 1750076.

[7] Bourada, F., Bousahla, A. A., Bourada, M., Azzaz, A., Zinata, A. and Tounsi, A. 2019. Dynamic investigation of porous functionally graded beam using a sinusoidal shear deformation theory. Wind and Structures. 28(1):19-30.

[8] Li, C., Shen, H. S. and Wang, H. 2019. Nonlinear vibration of sandwich beams with functionally graded negative Poisson's ratio honeycomb core. International Journal of Structural Stability and Dynamics. 19(03):1950034.

[9] Wu, H., Kitipornchai, S. and Yang, J. 2015. Free vibration and buckling analysis of sandwich beams with functionally graded carbon nanotube-reinforced composite face sheets. International Journal of Structural Stability and Dynamics. 15(07):1540011.

[10] Xu, G. D., Zeng, T., Cheng, S., Wang, X. H. and Zhang, K. 2019. Free vibration of composite sandwich beam with graded corrugated lattice core. Composite Structures. 229:111466.

[11] Li, M., Du, S., Li, F. and Jing, X. 2020. Vibration characteristics of novel multilayer sandwich beams: Modelling, analysis and experimental validations. Mechanical Systems and Signal Processing. 142:106799.

[12] Li, Y. H., Dong, Y. H., Qin, Y. and Lv, H. W. 2018. Nonlinear forced vibration and stability of an axially moving viscoelastic sandwich beam. International Journal of Mechanical Sciences. 138:131-145.

[13] Şimşek, M. and Al-Shujairi, M. 2017. Static, free and forced vibration of functionally graded (FG) sandwich beams excited by two successive moving harmonic loads. Composites Part B: Engineering. 108:18-34.

[14] Nguyen, T. K., Vo, T. P., Nguyen, B. D. and Lee, J. 2016. An analytical solution for buckling and vibration analysis of functionally graded sandwich beams using a quasi-3D shear deformation theory. Composite Structures. 156:238-252.

[15] Kahya, V. and Turan, M. 2018. Vibration and stability analysis of functionally graded sandwich beams by a multi-layer finite element. Composites Part B: Engineering. 146:198-212.

[16] Tossapanon, P. and Wattanasakulpong, N. 2016. Stability and free vibration of functionally graded sandwich beams resting on two-parameter elastic foundation. Composite Structures. 142:215-225.

[17] Arikoglu, A. and Ozkol, I. 2010. Vibration analysis of composite sandwich beams with viscoelastic core by using differential transform method. Composite Structures. 92(12):3031-3039.

[18] Pradhan, S. C. and Murmu, T. 2009. Thermo-mechanical vibration of FGM sandwich beam under variable elastic foundations using differential quadrature method. Journal of Sound and Vibration. 321(1-2):342-362.

[19] Mashat, D. S., Carrera, E., Zenkour, A. M., Al Khateeb, S. A. and Filippi, M. 2014. Free vibration of FGM layered beams by various theories and finite elements. Composites Part B: Engineering. 59:269-278.

[20] Nguyen, T. K., Nguyen, T. T. P., Vo, T. P. and Thai, H. T. 2015. Vibration and buckling analysis of functionally graded sandwich beams by a new higher-order shear deformation theory. Composites Part B: Engineering. 76:273-285.

[21] Vo, T. P., Thai, H. T., Nguyen, T. K., Inam, F. and Lee, J. 2015. A quasi-3D theory for vibration and buckling of functionally graded sandwich beams. Composite Structures. 119:1-12.

[22] Yang, Y., Lam, C. C., Kou, K. P. and Iu, V. P. 2014. Free vibration analysis of the functionally graded sandwich beams by a meshfree boundary-domain integral equation method. Composite Structures. 117:32-39.

[23] Mayandi, K. and Jeyaraj, P. 2015. Bending, buckling and free vibration characteristics of FG-CNT-reinforced polymer composite beam under non-uniform thermal load. Proceedings of the

Institution of Mechanical Engineers, Part L: Journal of Materials: Design and Applications. 229: 13-28.

[24] Mammano S.G. and Dragoni, E. 2017. Mechanical design of buckled beams for low-stiffness elastic suspensions: Theory and application. Proceedings of the Institution of Mechanical Engineers, Part L: Journal of Materials: Design and Applications. 231: 140-150.

[25] Alijani, A., Darvizeh, M. and Darvizeh, A. 2015. Elasto-plastic pre-and post-buckling analysis of functionally graded beams under mechanical loading. Proceedings of the Institution of Mechanical Engineers, Part L: Journal of Materials: Design and Applications. 229: 146-165.

[26] Majumdar, A. and Das, D. 2018. A study on thermal buckling load of clamped functionally graded beams under linear and nonlinear thermal gradient across thickness. Proceedings of the Institution of Mechanical Engineers, Part L: Journal of Materials: Design and Applications. 232: 769-784.

[27] Koissin, V., Shipsha, A., and Skvortsov, V. 2010. Effect of physical nonlinearity on local buckling in sandwich beams. Journal of Sandwich Structures & Materials.12: 477-494.

[28] Tran, T.T., Nguyen, N.H., Do, T.V., Minh,P.V. and Duc, N. D. 2019. Bending and thermal buckling of unsymmetric functionally graded sandwich beams in high-temperature environment based on a new third-order shear deformation theory. Journal of Sandwich Structures & Materials. 1099636219849268.

[29] Osofero, A.I., Vo, T.P., Nguyen, T-K. and Lee, J. 2016. Analytical solution for vibration and buckling of functionally graded sandwich beams using various quasi-3D theories. Journal of Sandwich Structures & Materials. 18: 3-29.

[30] Challamel, N. and Girhammar, U.A. 2011. Variationally-based theories for buckling of partial composite beam–columns including shear and axial effects. Engineering structures. 33: 2297-2319.

[31] Rahmani, M., Dehghanpour, S. and Barootiha, A. 2020. Free Vibration Analysis of Sandwich Beams with FG Face Sheets Based on the High Order Sandwich Beam Theory. Journal of Modern Processes in Manufacturing and Production. 9(2): 57-71.

[32] Rahmani, M., Mohammadi, Y., Kakavand, F. and Raeisifard, H. 2020. Vibration Analysis of Different Types of Porous FG Conical Sandwich Shells in Various Thermal Surroundings. Journal of Applied and Computational Mechanics. 6(3):416-432.

[33] Reddy, J.N. 2003. Mechanics of Laminated Composite Plates and Shells, Theory and Application. CRC Press, New York.

[34] Dariushi, S. and Sadighi, M. 2014. A new nonlinear high order theory for sandwich beams: An analytical and experimental investigation. Composite Structures. 108:779-788.

[35] Rahmani, M., Mohammadi, Y. and Kakavand, F. 2020. Buckling analysis of different types of porous fg conical sandwich shells in various thermal surroundings. Journal of the Brazilian Society of Mechanical Sciences and Engineering. 42(4):1-16.

[36] Rahmani, M. and Dehghanpour, S. 2021. Temperature-Dependent Vibration of Various Types of Sandwich Beams with Porous FGM Layers. International Journal of Structural Stability and Dynamics. 21(02):2150016.

[37] Mohammadi, Y. and Rahmani, M., 2020. Temperature-dependent buckling analysis of functionally graded sandwich cylinders. Journal of Solid Mechanics. 12(1):1-15.

[38] Rahmani M, Mohammadi Y. 2021. Vibration of two types of porous FG sandwich conical shell with different boundary conditions. Structural Engineering and Mechanics. 79(4):401-13.

[39] Şimşek, M. 2010. Fundamental frequency analysis of functionally graded beams by using different higher-order beam theories. Nuclear Engineering and Design. 240(4):697-705.

[40] Nguyen, T.K., Vo, T.P. and Thai, H.T. 2013. Static and free vibration of axially loaded functionally graded beams based on the first-order shear deformation theory. Composites Part B: Engineering. 55:147-157.

[41] Vo, T.P., Thai, H.T., Nguyen, T.K., Maheri, A. and Lee J. 2014. Finite element model for vibration and buckling of functionally graded sandwich beams based on a refined shear deformation theory. Engineering Structures. 64:12-22.